



Investigating *in vitro* and *in vivo* $\alpha\beta6$ integrin receptor-targeting liposomal alendronate for combinatory $\gamma\delta$ T cell immunotherapy



Naomi O. Hodgins^a, Wafa' T. Al-Jamal^b, Julie T.-W. Wang^a, Rebecca Klippstein^a, Pedro M. Costa^a, Jane K. Sosabowski^c, John F. Marshall^d, John Maher^e, Khuloud T. Al-Jamal^{a,*}

^a King's College London, Institute of Pharmaceutical Science, Franklin-Wilkins Building, 150 Stamford Street, London SE1 9NH, UK

^b School of Pharmacy, University of East Anglia, Norwich Research Park, Norwich NR4 7TJ, UK

^c Barts Cancer Institute, Queen Mary University of London, London EC1M 6BQ, UK

^d Centre for Tumour Biology, Barts Cancer Institute, Queen Mary University of London, London EC1M 6BQ, UK

^e King's College London, Division of Cancer Studies, Guy's Hospital, London SE1 9RT, UK

ARTICLE INFO

Keywords:

Integrin targeting
Bisphosphonates
 $\gamma\delta$ T cells
Liposomes
Immunotherapy

ABSTRACT

The $\alpha\beta6$ integrin receptor has been shown to be overexpressed on many types of cancer cells, resulting in a more pro-invasive and aggressive phenotype, this makes it an attractive target for selective drug delivery. In tumours that over-express the $\alpha\beta6$ receptor, cellular uptake of liposomes can be enhanced using ligand-targeted liposomes. It has previously been shown in both *in vitro* and *in vivo* studies that liposomal alendronate (L-ALD) can sensitise cancer cells to destruction by V γ 9V δ 2 T cells. It is hypothesised that by using the $\alpha\beta6$ -specific peptide A20FMDV2 as a targeting moiety for L-ALD, the therapeutic efficacy of this therapy can be increased in $\alpha\beta6$ positive tumours. Targeted liposomes (t-L) were formulated and the targeting efficacy of targeted liposomes (t-L) was assessed by cell uptake and cytotoxicity studies in the $\alpha\beta6$ positive cells line A375P $\beta6$. Bio-distribution of both L and t-L were carried out in $\alpha\beta6$ positive (A375P $\beta6$ and PANC0403) and $\alpha\beta6$ negative (A375Ppuro and PANC-1) subcutaneous tumour mouse models. Immuno-compromised mice bearing A375P $\beta6$ experimental metastatic lung tumours were treated with L-ALD or t-L-ALD as monotherapies or in combination with *ex vivo*-expanded V γ 9V δ 2 T cells. *In vitro*, $\alpha\beta6$ -dependant uptake of t-L was observed, with t-L-ALD being more effective than L-ALD at sensitising A375P $\beta6$ to $\gamma\delta$ T cells. Interestingly, t-L-ALD led to slightly higher but not significant reduction in tumour growth compared to L-ALD, when used as monotherapy *in vivo*. Moreover, both L-ALD and t-L-ALD led to significant reductions in tumour growth when used in combination with $\gamma\delta$ T cells *in vivo* but t-L-ALD offered no added advantage compared to L-ALD.

1. Introduction

Integrins are heterodimeric glycoproteins composed of non-covalently linked α and β subunits and are involved in a variety of cell processes including proliferation [1], survival [2], migration [3] and invasion [4], giving them a key role in cancer. The $\alpha\beta6$ integrin receptor is expressed on epithelia, usually only in the process of tissue remodelling [5] and wound healing [6]. However, overexpression of this receptor has been detected in many types of tumours including colon cancer [7], gastric carcinomas [8], oral squamous cell carcinomas [9] and breast cancer and is typically associated with a more pro-invasive and aggressive phenotype [10,11]. Therefore, this integrin provides an attractive molecular target for targeted drug delivery to cancer cells. The 20 amino acid peptide, A20FMDV2, (NAVPNLRGDLQVLAQKVART), derived from the VP1 coat-protein of

the foot-and-mouth disease virus, has shown very good specificity for $\alpha\beta6$ [12]. This peptide has been shown to effectively and specifically target $\alpha\beta6$ -expressing cancers [13]. A20FMDV2 has not previously been conjugated to any type of nanocarrier and its ability to target nanoformulations has not been tested. Only one other study has targeted the $\alpha\beta6$ integrin receptor using a nanoparticle formulation. In that study, liposomes were targeted using an alternative peptide, H2009.1 [14].

Alendronate (ALD), is a nitrogen containing bisphosphonate (N-BP) that can sensitise tumour cells to killing by V γ 9V δ 2 T cells in both *in vitro* [15–19] and *in vivo* studies [20–27]. The encapsulation of ALD in liposomes (L-ALD), has been shown to increase its therapeutic efficacy [24]. Long-circulating liposomes passively target the tumour due to the enhanced permeation and retention (EPR) effect [28], leading to a greater amount of the encapsulated drug reaching the tumour cells.

* Corresponding author.

E-mail address: khuloud.al-jamal@kcl.ac.uk (K.T. Al-Jamal).

<http://dx.doi.org/10.1016/j.jconrel.2017.04.025>

Received 14 December 2016; Received in revised form 31 March 2017; Accepted 17 April 2017

Available online 18 April 2017

0168-3659/© 2017 The Authors. Published by Elsevier B.V. This is an open access article under the CC BY license (<http://creativecommons.org/licenses/by/4.0/>).

The aim of this study is to formulate $\alpha\beta 6$ integrin targeted ALD liposomes (t-L-ALD), using the peptide A20FMDV2. It is hypothesised that A20FMDV2 conjugation to liposomal alendronate will promote $\alpha\beta 6$ -receptor mediated endocytosis and improved therapeutic efficacy in combination with $\gamma\delta$ T cell immunotherapy *in vitro* and possibly *in vivo*.

2. Materials and methods

Additional methods are described in Supplementary information.

2.1. Materials

1,2-distearoyl-*sn*-glycero-3-phosphocholine (DSPC) and 1,2-dipalmitoyl 1,2-distearoyl-*sn*-glycero-3-phosphoethanolamine-N-[methoxy (polyethylene glycol)-2000] (ammonium salt) (DSPE-PEG2000) were obtained from Lipoid (Germany). 1,2-dioleoyl-*sn*-glycero-3-phosphoethanolamine-N-(carboxyfluorescein) (CF-DOPE), 1,2-distearoyl-*sn*-glycero-3-phosphoethanolamine-N-diethylenetriaminepentaacetic acid (ammonium salt) (DSPE-DTPA) and DSPE-PEG(2000) maleimide were purchased from Avanti Polar Lipids, Inc. (USA). The cysteine-modified A20FMDV2 peptide (Sequence: NAVPNLRGLDQVLAQKVART-Cysteine, Purity: > 95%) was purchased from Genscript Limited (Hong Kong). Dextrose, cholesterol, sodium chloride, phosphate buffered saline (PBS) tablets, N-(2-Hydroxyethyl)piperazine-N'-(2-ethanesulfonic acid) (HEPES), methanol (Analytical reagent grade), chloroform (Analytical reagent grade), and Sepharose 2B were purchased from Sigma (UK). LavaPep™ Protein and Peptide quantification kit was obtained from Web Scientific (UK). PD-10 desalting column was obtained from GE Healthcare Life Sciences (UK). Snake Skin® dialysis tubing (MWCO 10000 Da) was purchased from Thermo-fisher (USA). Dulbecco's modified Eagle's medium (DMEM), Roswell Park Memorial Institute medium (RPMI), Glutamax™ and antibiotic-antimycotic solution were purchased from Invitrogen (UK). Foetal Bovine Serum was purchased from First Link (UK). Human AB serum (male) was obtained from Sigma (UK). Thiazolyl blue tetrazolium bromide (MTT), tropolone and alendronate sodium trihydrate were obtained from Alfa Aesar (UK). DMSO was obtained from Fisher (UK). Human IFN- γ ELISA Ready-set-go kit was purchased from eBiosciences (UK). The 10D5 antibody was obtained from Abcam (UK). FITC labelled secondary antibody was purchased from Cell Signalling (UK). D-Luciferin was obtained from Perkin Elmer (UK). Indium-111 chloride was obtained from Mallinckrodt (NL). Thin layer chromatography (TLC) strips for radiolabelling were purchased from Agilent Technologies UK Ltd. (UK). Isoflurane (IsoFlo®) for anaesthesia was purchased from Abbott Laboratories Ltd. (UK). All reagents were used without further purification.

2.2. Preparation of liposomes

Stock solutions of 40 mg/ml were prepared in chloroform/methanol (4:1 v/v). To avoid degradation, lipid solutions were stored at -20°C under nitrogen. Untargeted Liposomes (L) were prepared by thin film hydration (TFH). DSPC, cholesterol and DSPE-PEG2000 (55:40:5 molar ratio) were added to a 25 ml round-bottom flask and 2 ml chloroform/methanol (4:1 v/v) was added. A thin lipid film was formed upon removal of the solvent under reduced pressure using a rotary evaporator (Rotavapor® R-210, Buchi UK). The lipid film was flushed with nitrogen to remove any remaining traces of organic solvent. The film was then hydrated by adding 1 ml of PBS, adjusted to pH 7.4. The liposome suspension was left for 1 h at 60°C and was vortexed (Vortex genie 2, Scientific Industries Inc., USA) every 15 min [29]. Liposomes were prepared at a final concentration of 25 mM total lipid. The size and polydispersity (PDI) of the liposomes was reduced with serial extrusion using the mini-extruder (Avanti Polar Lipids, USA) through polycarbonate membranes (Avanti Polar Lipids, USA) with pore sizes

0.8 μm (5 \times), 0.2 μm (5 \times), 0.1 μm (10 \times) and 0.08 μm (15 \times) at 60°C . The resulting suspension was stored at 4°C .

For targeted liposomes (t-L), the liposomes were formed as above with the addition of 0.5–2%mol of DSPE-PEG₂₀₀₀-maleimide. The overall formulation of the liposomes was DSPC:cholesterol:DSPE-PEG₂₀₀₀:DSPE-PEG₂₀₀₀-maleimide (55:40:3–4.5:0.5–2 molar ratio). The DSPE-PEG₂₀₀₀ was reduced in order to keep the overall percentage of PEG2000 at 5%mol. After the liposomes were formed, they were flushed with nitrogen and incubated with A20FMDV2 peptide at RT overnight (25–100 μg peptide/ μmol lipid) under nitrogen. Excess peptide and ALD was removed by eluting the liposomes through a Sephadex 2B column with PBS; or *via* overnight dialysis against PBS using a dialysis bag with a MWCO of 10,000 kD at room temperature.

For cellular uptake studies, fluorescent liposomes were formed as above but with the inclusion of 1% mol CF-DOPE to give a final liposome composition of DSPC:CF-DOPE:cholesterol:DSPE-PEG₂₀₀₀:DSPE-PEG₂₀₀₀-maleimide (54:1:40:4:1 molar ratio).

Liposomes containing alendronate (L-ALD and t-L-ALD) were prepared as above, but the lipid film was hydrated with 1 ml of 100 mM solution of ALD in HEPES Buffered Saline (HBS, 20 mM HEPES, 150 mM NaCl). Un-encapsulated ALD was removed by overnight dialysis against HBS using a dialysis bag with a MWCO of 10,000 kD.

2.3. Peptide quantification

The amount of peptide conjugated to the liposomes was determined by LavaPep™ Protein and Peptide quantification kit. A calibration curve was obtained in the range 0.122–500 $\mu\text{g}/\text{ml}$ using free A20FMDV2. Liposomes were diluted 100 times in deionised water and the amount of peptide quantified according to the manufacturer's instructions. Briefly, 50 μl of the diluted sample was incubated with 50 μl of LavaPep working solution for 60 min in the dark at RT. The fluorescence intensity was then measured using 540 ± 10 nm and 630 ± 10 nm excitation and emission filters, respectively (FLUOStar Omega, BMG Lab Tech). The per cent peptide conjugated to the liposomes was calculated by quantifying the amount of peptide in the liposome sample before and after purification.

2.4. Cell culture conditions

The cell lines PANC-1 (CRL-1469™, pancreatic), PANC0403 (CRL-2555™, pancreatic) and 4T1 (CRL-2539™, breast) were obtained from ATCC®. A375Ppuro and A375P $\beta 6$ puro cell lines were created using the human melanoma cell line A375P (CRL-3224™, melanoma), which was infected with pBabe retroviruses encoding puromycin resistance alone or in combination with cDNA for human $\beta 6$, as previously reported [12]. The A375Ppuro and A375P $\beta 6$ cell lines were a kind gift from Prof. John Marshall (QMUL). The A375P $\beta 6$ cell line was subsequently transfected with firefly luciferase (luc) using an SFG retroviral vector whereby luc was co-expressed with dsTomato red fluorescent protein. Transduced cells were then flow sorted for red fluorescence to obtain a pure A375P $\beta 6$ -luc cell line [24]. All cell lines were maintained at 37°C , 5% CO_2 and 5% relative humidity. Advanced RPMI (PANC-1, PANC0403, 4T1) or DMEM media (A375Ppuro, A375P $\beta 6$ puro) were used, both of these were supplemented with 10% FBS, 1% GlutaMAX™ and 1% Penicillin/Streptomycin.

2.5. Characterisation of cell lines for $\alpha\beta 6$ integrin expression

$\alpha\beta 6$ integrin receptor expression was confirmed by 10D5 antibody staining and flow cytometry. Cells ($1 \times 10^5/100 \mu\text{l}$) were incubated with 5 μl of 10D5 or the isotype control (IgG FITC) for 30 min at 4°C , washed twice with 1 ml PBS before 30 min incubation with 2.5 μl of the FITC labelled IgG secondary antibody at 4°C then washed with PBS. Using the FL1 detector, 10,000 cells were gated and the fluorescence was analysed under live gating. The cells were read on a BD FACS

Calibur™ flow cytometer obtained from BD Bioscience (US) and analysed using FlowJo software.

2.6. Cellular uptake of liposomes using flow cytometry

Cells were plated in a 24 well plate at a density of 50,000 cells/well and left overnight to allow the cells to attach. Cells were treated with 32.5–130 μM CF-DOPE containing liposomes (L or t-L) in complete media (10% FBS) for 1 or 4 h. In order to determine if the increased uptake of t-L was $\alpha\beta 6$ receptor specific, peptide inhibition studies were carried out. Cells were incubated at 4 °C for 10 min and were then treated with 0.2 ml of 50 $\mu\text{g}/\text{ml}$ free peptide in complete media for a further 10 min on ice. The fluorescently labelled L and t-L (32.5–130 μM) were then additionally incubated with the cells for 1 or 4 h. Additional peptide (50 μg in 25 μl PBS) was added after 1 h to ensure that the $\alpha\beta 6$ receptors remained blocked. Upon completion of the incubation period, the cells were washed with PBS, trypsinised and transferred into BD flow cytometer tubes. The cells were washed in PBS and re-suspended in 500 μl of PBS. The fluorescence was analysed in triplicates for each condition using the FL1 detector with 10,000 cells gated. All flow cytometry data was acquired using a BD FACS Calibur™ flow cytometer obtained from BD Bioscience (US) and analysed using FlowJo software.

2.7. Treatment of cancer cell lines with L-ALD/t-L-ALD and $\gamma\delta$ T cells in combination therapy studies

The cell lines A375Ppuro, A375P $\beta 6$, PANC-1 and PANC0403 were seeded at 50,000 cells/well in 96 well plates. Cells were treated for 24 h with 30 or 60 μM of ALD, L-ALD or t-L-ALD. Empty-liposomes (EL) and targeted EL (t-EL) were used as controls at lipid concentrations equivalent to that of the L-ALD and t-L-ALD, depending on the drug loading. The treatments were removed and replaced with 2.5×10^5 *ex vivo* expanded V $\gamma 9\text{V}\delta 2$ T cells, or $\gamma\delta$ T cell culture media as a control, for a further 24 h. The $\gamma\delta$ T cells were then removed and the cell monolayers were washed with PBS before cell viability was assessed with MTT as described below.

2.8. MTT assay

MTT (3-(4,5-dimethylthiazol-2-yl)-2,5-diphenyltetrazolium bromide) solution was prepared in PBS at a concentration of 5 mg/ml and was diluted in media (1:6) prior to use. The supernatant of each well was removed and MTT solution (120 μl) was added to each well. The plates were then incubated at 37 °C and 5% relative humidity for 3 h. The MTT solution from each well was removed and DMSO (200 μl /well for 96 well) was added and incubated for 5 min at 37 °C, to eliminate air bubbles. The absorbance was read at 570 nm with reference at 630 nm (FLUOStar Omega, BMG Lab Tech). Percentage cell survival was determined by calculating the absorbance of treated cells as a percentage of that of untreated cells.

2.9. Determination of IFN- γ concentration by ELISA

Supernatant from the co-culture assay was removed from each of the wells immediately before the cytotoxicity assay was performed. The supernatant was centrifuged to remove the $\gamma\delta$ T cells and was stored at –80 °C until required. Supernatants were diluted 1:40 and analysed using a human IFN- γ ELISA Ready-set-go-kit as per the manufacturer's protocol.

2.10. Radiolabelling of DTPA containing liposomes

DTPA containing liposomes were prepared with the TFH method as above but with 1% of the DSPC replaced with 1% molar ratio of DSPE-DTPA, and radiolabelled with ^{111}In [30]. The required volume of ^{111}In ,

containing 1 MBq per mouse for bio-distribution studies or 10–15 MBq per mouse for imaging studies was added to 2 M ammonium acetate buffer (one-ninth of the reaction volume, pH 5.5). This was then added to the liposome sample (100 μl of 20 mM liposomes/mouse) to give a final ammonium acetate concentration of 0.2 M, and incubated for 30 min at RT. The reaction was quenched by the addition of 0.1 M EDTA solution to the mixture (5% v/v of the reaction mixture) to chelate free ^{111}In . Unbound ^{111}In :EDTA was removed using NAP-5 desalting columns equilibrated with PBS and the liposomes were collected in fraction 1–3 (~150 μl per injection dose).

2.11. Efficiency and stability of the radiolabelling in serum

Samples of the radiolabelled liposomes or ^{111}In :EDTA were spotted in glass microfibre chromatography paper impregnated with silica gel. These strips were then developed using a mobile phase of 50 mM EDTA in 0.1 M ammonium acetate. Strips were placed on a multi-purpose storage phosphor screen (Cyclone®, Packard, Japan) and kept in an autoradiography cassette (Kodak Biomax Cassette®) for 10 min. Quantitative autoradiography counting was then carried out using a cyclone phosphor detector (Packard®, Australia). The labelling stability was tested by incubation of the radio-conjugates in the presence or absence of FBS. Samples were diluted in 50% FBS or PBS [1:2 (v/v)], and incubated for 24 h at 37 °C. The percentage of ^{111}In :EDTA (immobile spot) remained conjugated to the liposomes was evaluated by TLC, using the same protocol as described above.

2.12. Animal models

All animal experiments were performed in compliance with the UK Home Office (1989) Code of Practice for the housing and care of Animals used in Scientific Procedures. Female SCID/Beige (SPECT/CT studies) and male NOD SCID gamma (NSG) mice (bio-distribution and therapy studies), 4–6 weeks old, were obtained from Charles River (UK). Female BALB/c mice, 4–6 weeks old, were obtained from Harlan Laboratories (UK). For the human xenograft tumour models, subcutaneous (s.c.) tumours were established by injecting 5×10^6 cells in 100 μl PBS into each of the rear-flanks of SCID/Beige. For the murine tumour model, 1×10^6 cells in 100 μl PBS were injected into each of the rear flanks of BALB/c mice. The size of the tumour was measured using callipers and tumour volume were determined using the equation:

$$\text{Tumour Volume}(\text{mm}^3) = (A^2 B \pi) / 6$$

where A and B represent the width and the length of the tumours, respectively [31]. Experiments commenced when tumours reached ~300 mm^3 . For the lung model, 5×10^5 cells were injected into the tail vein of NSG mice. This tumour model was monitored *via* s.c. injection of the mice with 100 μl 30 mg/ml luciferin/20 g mouse and subsequent scanning after 20 min using an IVIS Lumina series III *In Vivo* Imaging system (Perkin-Elmer). Images were quantitatively analysed by drawing regions of interest (ROI) around the tissues using Living Image 4.3.1 Service Pack 2 software (Perkin-Elmer, USA).

2.13. Whole body SPECT/CT imaging of radiolabelled liposomes in tumour-bearing mice

Mice were injected with liposomes containing 2 μmol lipid and radiolabelled with 1 MBq or 10–15 MBq, for bio-distribution and SPECT/CT studies, respectively, *via* tail vein injection. Mice were imaged with nanoSPECT/CT scanner (Bioscan®, USA) 0–30 min, 4 h and 24 h post *i.v.* injection. For each mouse, a tomography was initially performed (45 Kvp; 1000 ms) to obtain parameters required for the SPECT and CT scanner, including the starting line, finish line and axis of rotation of the acquisition for each mouse. SPECT scans were obtained using a 4-head scanner with 1.4 mm pinhole collimators and the

following settings: number of projections: 24; time per projection: 60 s and duration of the scan 60 min. CT scans were obtained at the end of each SPECT acquisition using 45 Kvp. All data were reconstructed with MEDISO (medical Imaging System) and the combining of the SPECT and CT acquisitions were performed using PMOD® software.

2.14. Gamma counting of radiolabelled liposomes in tumour-bearing mice

After 24 h, the mice were perfused with ~25 ml of 1000 U/l heparin in 0.9% sodium chloride in order to remove any liposomes remaining in the blood. The major organs (brain, lung, liver, spleen, kidney, heart, stomach and intestine), muscle, skin, bone (femur), carcass and tumours were collected, weighed and placed in scintillation vials. Additionally, 5 µl blood samples taken at various time points (5, 10, 30, 60, 240 and 1440 min), and urine and faeces collected with the aid of metabolic cages were also placed in scintillation vials for analysis. Each sample was analysed for [¹¹¹In] specific activity using an automated gamma counter (LKB Wallac 1282 Compugamma, PerkinElmer, UK) together with dilutions of injected dose with dead time limit below 60%. The gamma rays emitted by the radioisotope were detected, quantified and corrected for physical radioisotope decay by the gamma counter. Radioactivity readings (counts per minute - CPM) were plotted as percentage of injected dose per organ or percentage of injected dose per gram of tissue.

2.15. Therapy study

Male NSG mice (4–6 weeks) were inoculated with 5×10^6 A375Pβ6.luc cells by i.v. injection to form experimental metastatic lung tumours. Bioluminescence imaging of mice was carried out on day 6 as described above and mice were divided into 4 treatment groups: naïve, L-ALD, γδ T cells and L-ALD and γδ T cells combination treatment. Doses used in therapy experiments were 0.5 µmol of ALD/mouse (L-ALD) and 1×10^7 cells/mouse (γδ T cells), all injected *via* the tail vein. Three doses of each treatment were given at one-week intervals on dates 7, 14 and 21. In the case of the combination treatment, mice were pre-injected with L-ALD (days 6, 13, and 20) then injected with γδ T cells (days 7, 14, and 21). Tumour growth was monitored by bioluminescence imaging twice weekly, as described above.

2.16. Determination of IFN-γ concentration with ELISA

Animals from the therapy study were sacrificed and sera was analysed for human IFN-γ. Sera were diluted 1:2 and analysed using a human IFN-γ ELISA Ready-set-go-kit as per the manufacturer's protocol.

2.17. Pre-incubation of liposomes with mouse sera

Mouse serum was obtained by allowing blood obtained from a terminal bleed of SCID/Beige mice to clot. The blood was centrifuged to pellet the clotted cells, and the serum was removed for further use. t-L were incubated with the mouse serum for various periods of time (10 min, 1 h, 4 h) at 37 °C. Any proteins that had not interacted with the surface of the liposomes were removed using a 10 cm Sepharose 2B column and eluted using PBS. t-L were incubated with cells without any further processing and their uptake analysed by flow cytometry as described above.

2.18. Statistics

For all experiments, data were presented as mean ± SD, except for therapy experiments where data were presented as mean ± SEM; *n* denotes the number of repeats. Independent variable Student *t*-tests were performed using IBM SPSS version 20 for *in vitro* cytotoxicity

Table 1
Physicochemical characteristics of liposomes with or without peptide.

Initial peptide added (µg/µmol lipid) ^a	Size (nm) ^{b,d}	PDI ^{b,d}	Zeta Potential (mV) ^{c,d}
0	159.1 ± 1.7	0.098 ± 0.025	-14.6 ± 1.53
25	157.8 ± 2.5	0.08 ± 0.013	-12.5 ± 1.08

^a Liposomes containing 1% mol DSPE-PEG₂₀₀₀-maleimide.

^b Hydrodynamic diameter measured by dynamic light scattering.

^c Analysed by electrophoretic light scattering using 10 mM NaCl.

^d Data are represented as mean ± SD.

studies. For *in vivo* studies, significant differences were examined using one-way ANOVA. The *t*-value, degrees of freedom and two-tailed significance (*p*-value) were determined. **p* < 0.05, ***p* < 0.01 and ****p* < 0.001.

3. Results

3.1. Preparation and characterisation of αvβ6 integrin-targeted liposomes (t-L)

DSPC:Chol:DSPE-PEG₂₀₀₀ liposomes were prepared using lipid film hydration method and extrusion. t-L were prepared by incorporating DSPE-PEG₂₀₀₀-maleimide (0.5–2 mol%) in the liposomes, then linked directly to αvβ6-targeting peptide. Free peptide was removed before further characterisation. The effects of %mol DSPE-PEG₂₀₀₀-maleimide and the peptide A20FMDV2 (25 µg/µmol lipid) on the physicochemical characteristics of the liposomes were examined. There was no significant difference in the hydrodynamic size (157.8–159.1 nm), PDI (0.080–0.098) or zeta potential (-12.5 to -14.6 mV) of the liposomes when DSPE-PEG₂₀₀₀-maleimide (1 mol%) or A20FMDV2 were included in the formulation (Table 1). The size of the liposomes is in the range reported to be extravasated in regions of leaky vasculature as part of the EPR effect [32]. The low PDI values indicated that the liposomes were homogenous in size and the absence of liposome aggregation. The identical physicochemical characteristics of the L and t-L ensure that any differences in behaviour of these liposomes are solely due to the ability of the A20FMDV2 peptide to bind to the αvβ6 integrin receptor. Liposomes containing 0.5 or 2% DSPE-PEG₂₀₀₀-maleimide with or without A20FMDV2 were also characterised and no significant change to the physicochemical characteristics of the liposomes were observed (Table S1).

3.2. Optimisation of peptide loading on liposomes surface

The effect of different initial addition of peptide on the final peptide loading on the t-L was examined. The LavaPep peptide assay was used to quantify the amount of peptide conjugated to the t-L and confirmed the purification of the t-L from the unconjugated A20FMDV2 using a Sepharose 2B column (Fig. S1). In the case of 1%mol DSPE-PEG₂₀₀₀-maleimide, the amount of A20FMDV2 added to the liposomes was adjusted from 25 to 100 µg per µmol lipid (10–40 nmol per mol lipid) (Table 2). Final peptide loading achieved ranged from 17.7 to 21.7 µg peptide/µmol lipid. There was no significant difference between the amount of A20FMDV2 added and the final peptide loading so it was therefore decided to use 25 µg peptide per µmol lipid (initial peptide loading) to prepare the t-L for subsequent studies. Additionally, when the %mol DSPE-PEG₂₀₀₀-maleimide was adjusted (0.5 or 2 mol%), the amount of peptide loaded onto the liposomes increased proportionally to the % of DSPE-PEG₂₀₀₀-maleimide included in the liposome formulation (Table S2). All t-L used for *in vitro* and *in vivo* experiments contained 1% mol DSPE-PEG₂₀₀₀-maleimide, as initial experiments determined that no improvement in targeting efficacy was observed when the DSPE-PEG₂₀₀₀-maleimide content was increase to 2% mol (Figs. S2 and S3).

Table 2
Optimisation of peptide loading on liposomes.

Initial peptide added ($\mu\text{g}/\mu\text{mol}$ lipid) ^a	Final peptide loading ($\mu\text{g}/\mu\text{mol}$ lipid) ^{b,d}	nmol peptide/ μmol lipid ^{b,d}	% Peptide conjugated ^{c,d}
25	21.7 \pm 4.5	8.5 \pm 1.8	84.8 \pm 17.6
50	17.7 \pm 4.6	6.9 \pm 1.8	34.5 \pm 8.9
100	21.2 \pm 0.9	8.3 \pm 0.4	20.67 \pm 0.9

^a Liposomes containing 1% mol DSPE-PEG₂₀₀₀-maleimide.

^b Determined by LavaPep Peptide quantification kit.

^c Calculated as a percentage of initial peptide added.

^d Data are represented as mean \pm SD.

3.3. *In vitro* targeting of t-L is $\alpha\text{v}\beta 6$ integrin expression dependant

The targeting efficacy of the liposomes was examined by looking at the uptake of fluorescently-labelled L and t-L in $\alpha\text{v}\beta 6$ positive (A375P $\beta 6$, 4T1 and PANC0403) and negative (A375Ppuro and PANC-1) cell lines. The results are displayed as mean fluorescence intensity (MFI) ratio of t-L to L. When a value of 1 is obtained the uptake of L and t-L were the same. A value of > 1 indicates that the t-L was taken up in greater quantities than L, and that a positive targeting effect has occurred. All experiments were carried out in media containing 10% foetal bovine serum (FBS), as the large increase in internalisation of both L and t-L by starved cells in serum-free media masked any targeting effect of t-L (Fig. S4).

To evaluate the targeting efficiency of t-L, three $\alpha\text{v}\beta 6$ integrin positive cell lines were used. These were the $\alpha\text{v}\beta 6$ integrin-transfected human melanoma cell line A375P $\beta 6$ and two cell lines that naturally express $\alpha\text{v}\beta 6$: the human pancreatic cancer cell line, PANC0403 and the murine breast cancer cell line 4T1. The antibody 10D5 was used to measure the expression of $\alpha\text{v}\beta 6$ integrin receptor on the panel of cancer cell lines used. As seen in Fig. 1, 4T1 cells expressed the lowest amount of $\alpha\text{v}\beta 6$ integrin receptor, while higher expression was seen in PANC0403 and A375P $\beta 6$ cells. A correlation between the extent of $\alpha\text{v}\beta 6$ integrin receptor expression on the surface of cells and the fold increase of t-L uptake compared to L could be seen. A375P $\beta 6$ and PANC0403 showed a significantly higher fold increase of t-L/L compared to 4T1 ($p < 0.01$) at both 1 and 4 h. Additionally, at 4 h, A375P $\beta 6$ demonstrated enhanced uptake of t-L/L compared to PANC0403 ($p < 0.05$). These data demonstrate the $\alpha\text{v}\beta 6$ integrin-specific targeting effect of the liposomes. The results also suggest that a certain level of expression of the receptor is required for targeting to occur.

3.4. Uptake of t-L in $\alpha\text{v}\beta 6$ expressing cells is inhibited with the free peptide A20FMDV2

To further prove that enhanced liposomal targeting efficiency was related to the interaction between the peptide in t-L and the $\alpha\text{v}\beta 6$ integrin receptor, peptide inhibition studies were carried out in the presence of excess A20FMDV2. Fig. 2 displays the results obtained from the melanoma and pancreatic cancer paired cell lines. A 1.5- to 2-fold increase in the uptake of t-L compared to L was seen at both 1 and 4 h for the $\alpha\text{v}\beta 6$ positive cell line, A375P $\beta 6$ (Fig. 2B). However, enhancement of liposomal uptake was significantly reduced in the presence of the free A20FMDV2 ($p < 0.05$) with a ratio of ~ 1 obtained when compared with untargeted liposomes. A similar trend was observed for the $\alpha\text{v}\beta 6$ positive PANC0403 cell line, whereby, when the cells were incubated with A20FMDV2, a lowering of the fold increase in liposomal uptake could be seen ($p < 0.05$) (Fig. 2C). This further indicates that the increased amount of t-L taken up by the cells in relation to L is $\alpha\text{v}\beta 6$ receptor-dependent. The $\alpha\text{v}\beta 6$ negative cell lines, A375Ppuro and PANC-1, (Fig. S5) were also used to further confirm the specificity of the t-L. PANC-1 took up equal amounts of L and t-L and this did not

change in the presence of free A20FMDV2. For A375Ppuro, a small increase in the amount of t-L when compared to L was observed in some conditions and was affected by the presence of A20FMDV2, despite their lack of the integrin receptor. This t-L/L ratio was lower than that of $\alpha\text{v}\beta 6$ positive cell lines, however, and only occurred sporadically.

3.5. t-L-ALD are more effective than L-ALD at sensitising an integrin positive cell line to destruction by $\gamma\delta$ T cells

In order to test the therapeutic benefit of using liposomes targeted with the A20FMDV2 peptide, ALD was encapsulated into L and t-L formulations. The ability of the resulting L-ALD and t-L-ALD to sensitise cancer cell lines to destruction by V γ 9V δ 2 T cells was then tested by assessing cell viability and $\gamma\delta$ T cell-derived IFN- γ production. The $\alpha\text{v}\beta 6$ positive cell line A375P $\beta 6$ was used in this assay. As shown in Fig. 3, none of the treatments in isolation caused toxicity. However, when the cells were pre-treated with free or liposomal ALD, and were subsequently treated with $\gamma\delta$ T cells, a significant decrease in cell viability was observed. t-L-ALD in combination with $\gamma\delta$ T cells led to significantly lower cell viability than L-ALD at both 30 μM ($p < 0.001$) and 60 μM ($p < 0.01$) concentrations. To further confirm the increased sensitivity of $\alpha\text{v}\beta 6$ positive cancer cells to $\gamma\delta$ T cells when treated with t-L-ALD as compared to L-ALD, the IFN- γ release from the $\gamma\delta$ T cells was quantified. Significantly higher amounts of IFN- γ were released when the $\gamma\delta$ T cells were co-cultured with cells pre-treated with t-L-ALD as compared to L-ALD ($p < 0.001$ and $p < 0.001$ for 30 μM and 60 μM , respectively). This finding is in agreement with the results obtained by the MTT assay. In the case of the $\alpha\text{v}\beta 6$ negative cell line, A375Ppuro, no difference in the ability of L-ALD and t-L-ALD to sensitise the cells to $\gamma\delta$ T cells was seen in terms of either cytotoxicity or IFN- γ release (Fig. S6).

3.6. Whole body SPECT/CT imaging of mice injected with ¹¹¹In labelled L and t-L

L and t-L were formulated with 1% mol DSPE-DTPA and radiolabelled with ¹¹¹In. Labelling efficiencies of 86.3% and 61.9% were obtained for L and t-L, respectively (Fig. S7). Stability studies were performed after 24 h at 37 °C in both PBS and 50% FBS in order to replicate *in vivo* conditions. For L, 87.8% of the ¹¹¹In remained bound to the liposomes after 24 h incubation with PBS. On incubation of L with serum, 91% stability was seen. For t-L, 80.7% and 78.2% of ¹¹¹In remained bound after 24 h incubation with PBS and FBS, respectively.

Tumour-bearing SCID/Beige mice were imaged by SPECT with computed tomography (CT) scanning to study the organ bio-distribution of radiolabelled L and t-L. The mice were inoculated with either the two melanoma or the two pancreatic human xenograft models on their back left flank ($\alpha\text{v}\beta 6$ negative tumour: A375Ppuro or PANC-1) (right of the image) or right flank ($\alpha\text{v}\beta 6$ positive tumour: A375P $\beta 6$ or PANC0403) (left of the image). They were imaged immediately after injection, and 4 and 24 h post-injection by SPECT/CT. As shown in Fig. 4, no differences in the whole body bio-distribution for [¹¹¹In]L and [¹¹¹In]t-L were observed. At early time-points, good blood circulation was observed for both types of liposomes as indicated by signals seen in the heart and head of the mice. Over time, the liposomes accumulated in the liver and spleen. Slight accumulation of the liposomes in the tumours could also be seen at later time-points, but this could not be clearly observed in these images, possibly due to masking by prolonged blood circulation of the liposomes. L and t-L gave comparable signals in both the positive and negative tumours. Gamma counting was used to quantify the tumour uptake of L and t-L.

3.7. Comparable tumour distribution for both L and t-L was obtained in integrin negative and positive models

The organ bio-distribution and tumour uptake of [¹¹¹In]L and

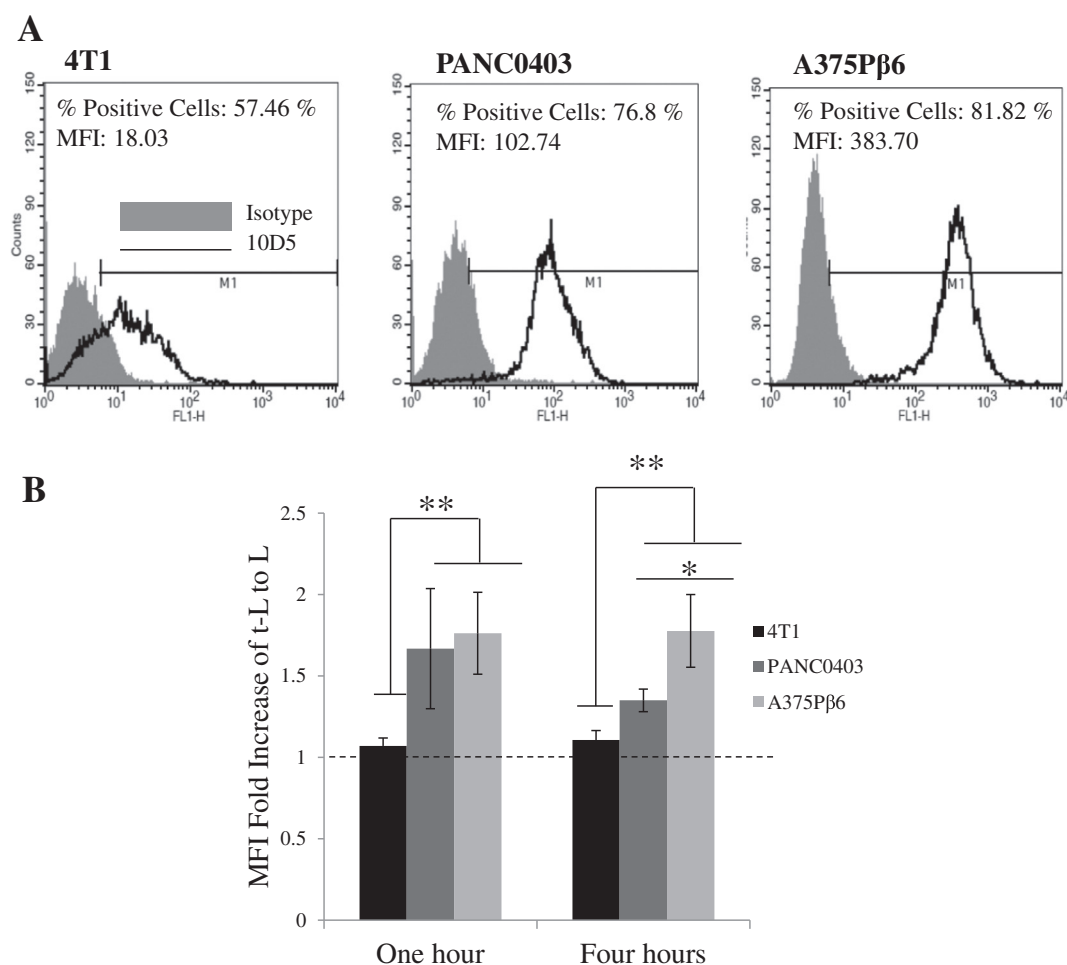


Fig. 1. The effect of the extent of expression of $\alpha\text{v}\beta 6$ integrin receptor on the uptake of t-L. (A) Representative images of cell lines incubated with the antibody 10D5 (specific to $\alpha\text{v}\beta 6$) or an isotype control. Cells were analysed for $\alpha\text{v}\beta 6$ integrin receptor expression using flow cytometry and FL-1 detector. In a comparison of the $\alpha\text{v}\beta 6$ expression of different cell lines using the % positive cells gated in M1 or the MFI, the 4T1 cancer cell line showed the lowest receptor expression, while A375Pβ6 has the highest expression both in terms of % of positive cells and the number of receptors per cell. (B) Comparison of the MFI fold increase of fluorescently labelled t-L to L. Cells were treated with 32.5 μM L or t-L for 1 or 4 h. With increasing expression of $\alpha\text{v}\beta 6$, the uptake of t-L in relation to L further increases. This is a further indication of the specificity of the t-L to the $\alpha\text{v}\beta 6$ integrin receptor. Values are expressed as mean \pm SD ($n = 3$). * $p < 0.05$, ** $p < 0.01$ (ANOVA).

[^{111}In]t-L in tumour-bearing SCID/Beige mice, was then quantitatively determined by gamma counting. No significant differences were observed in the blood circulation profiles of [^{111}In]L and [^{111}In]t-L (Fig. 5A). At 1 h post administration, $\sim 66\%$ ID of both formulations remained in the blood, decreasing to 31–39%ID and $\sim 8\%$ ID after 4 and 24 h, respectively. L and t-L also had similar excretion profiles (Fig. 5B), with only small fraction of the liposomes excreted within 24 h in the urine (1.0–1.5%ID) and faeces (0.30–0.37%ID). In agreement with the SPECT imaging studies, liposomes accumulated mainly in the liver (L: $43 \pm 3\%$ ID/g t-L: $29 \pm 9\%$ ID/g) and the spleen (L: $255.5 \pm 89.7\%$ ID/g t-L: $219.4 \pm 78.8\%$ ID/g) (Figs. 5C and S8). No significant differences in the organ bio-distribution of [^{111}In]L and [^{111}In]t-L were observed. Additionally, no difference in uptake of t-L and L was observed in the $\alpha\text{v}\beta 6$ positive tumours. A comparison of the uptake of both [^{111}In]L and [^{111}In]t-L among the different tumour models showed that when the tumours were normalised by weight, there was no significant difference in the uptake of the liposomes among different tumour models (1.7–3.2%ID/g tumour). Once again no difference in bio-distribution was observed between [^{111}In]L and [^{111}In]t-L.

3.8. Both L-ALD and t-L-ALD sensitise tumours to $\gamma\delta$ T cell therapy in vivo

L-ALD and t-L-ALD were used as a monotherapy and in combination

with *ex vivo*-expanded V γ 9V δ 2 T cells in an experimental metastatic lung model with the $\alpha\text{v}\beta 6$ positive A375Pβ6 melanoma cell line in NOD-SCID gamma (NSG) mice. On day 6, all six groups had the same average tumour size ($\sim 1.3 \times 10^6$ photons, as determined by bioluminescence imaging). L-ALD, t-L-ALD or $\gamma\delta$ T cells as monotherapies did not result in a significant reduction in tumour growth. Monotherapy with t-L-ALD showed a trend towards greater effectiveness than L-ALD ($4.70 \times 10^8 \pm 1.78 \times 10^8$ vs. $1.24 \times 10^9 \pm 4.65 \times 10^8$ photons, day 27, $p = 0.15$). However, this difference was not significant due to variability in tumour size. Mice pre-treated with L-ALD or t-L-ALD 24 h prior to injection of $\gamma\delta$ T cells showed a significant reduction in tumour growth, with tumour sizes of $7.53 \times 10^7 \pm 2.02 \times 10^7$ and $9.06 \times 10^7 \pm 3.33 \times 10^7$ photons, respectively, compared to $1.42 \times 10^9 \pm 6.38 \times 10^8$ photons for naïve tumours on day 27 (Fig. 6). No improvement on the ability of t-L-ALD to sensitise the tumours to $\gamma\delta$ T cells compared to L-ALD was observed. IFN- γ serum levels were measured on day 27. Mice pre-treated with L-ALD or t-L-ALD prior to $\gamma\delta$ T cells had levels of 32.6 ± 19.3 and 12.3 ± 4.4 pg/ml ($p < 0.05$), respectively, compared to only 6.5 ± 0.9 pg/ml in $\gamma\delta$ T cells-only treated group, mirroring the significant reduction in tumour growth observed in these groups.

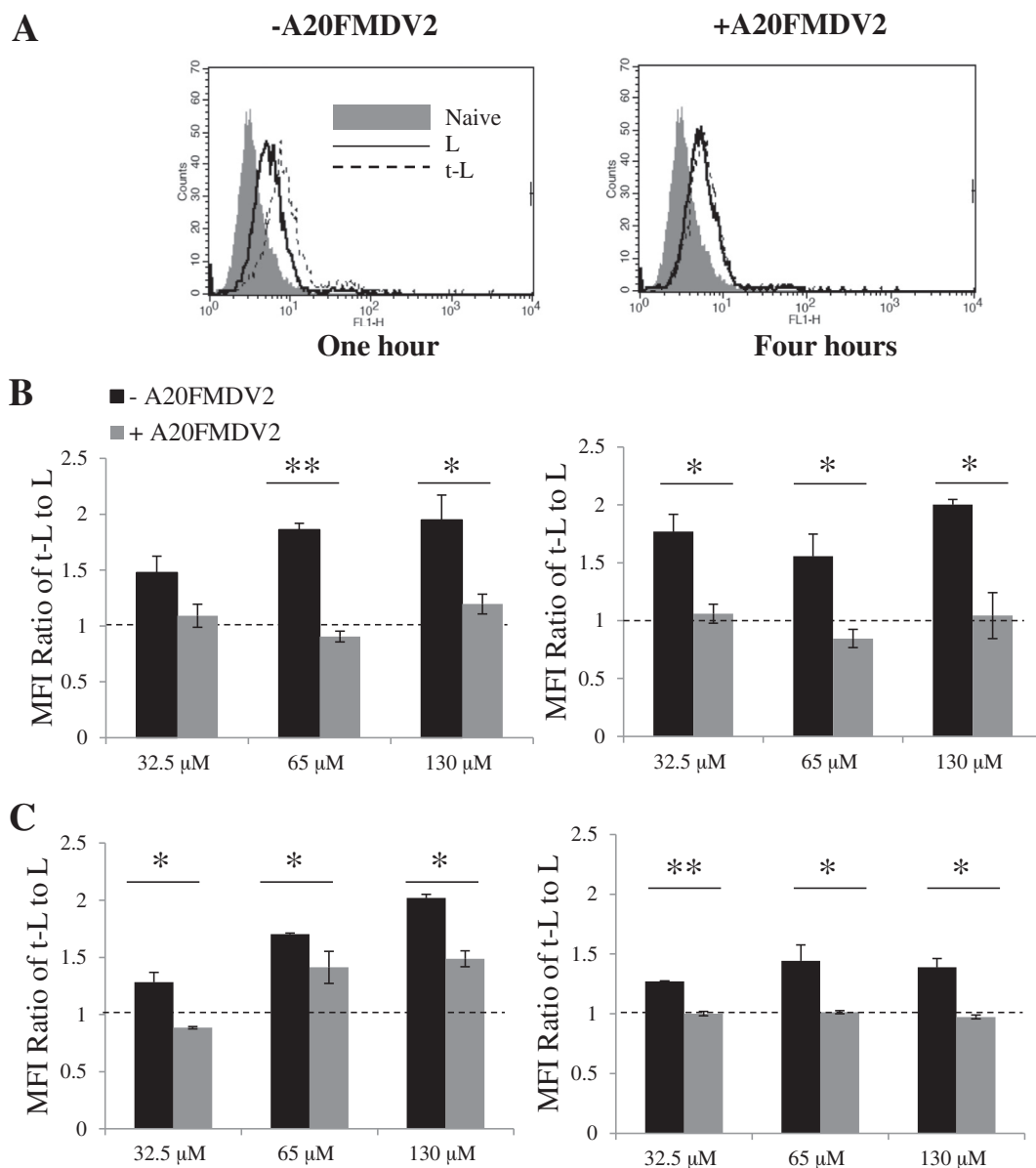


Fig. 2. Cellular uptake of fluorescent liposomes in $\alpha v \beta 6$ positive cancer cell lines *in vitro*. A375P $\beta 6$ and PANC0403 cells were incubated with L or t-L labelled with 1 mol% CF-DOPE for either 1 or 4 h. Cells were pre-treated on ice with either normal media (black bars) or media containing 50 μ g/ml (grey bars) of the free A20FMDV2 peptide for 10 min prior to addition of the liposomes. Cellular uptake was assessed by measuring the mean fluorescence intensity (MFI) using flow cytometry (A) Flow cytometry plots demonstrate the reduction in t-L uptake in A375P $\beta 6$ cells in the presence of free A20FMDV2. (B) A375P $\beta 6$ showed reduced uptake of t-L when incubated with free A20FMDV2 at both 1 and 4 h. (C) Similarly, PANC0403 cells also showed a reduction in targeting ability of t-L when incubated with free A20FMDV2. * $p < 0.05$, ** $p < 0.01$ (Student's *t*-test + A20FMDV2 vs. -A20FMDV2).

3.9. Use of mouse sera in cell uptake studies reduces receptor-mediated cell uptake of t-L *in vitro*

In order to explore one possible explanation for the lack of improvement in therapeutic efficacy of t-L-ALD compared to L-ALD when used in combination with $\gamma \delta$ T cells in therapy studies, cell uptake studies were performed *in vitro*, whereby t-L were pre-incubated with mouse serum and excess serum and unbound proteins were removed by size exclusion chromatography, prior to their 1 h incubation with cell lines (Fig. 7). Interestingly, this study showed the reduction in receptor-mediated uptake was indeed dependent on the incubation times with mouse serum. This result suggests that mouse serum played a direct role in reducing active targeting efficiency *in vivo*. Unfortunately, whether this was a direct effect of the enzymes present in the serum on A20FMDV2 peptide's stability or a protein corona effect, could not be precisely established.

4. Discussion

In our study, $\alpha v \beta 6$ positive cells were successfully targeted *in vitro*. Higher uptake of t-L *versus* L was observed in the A375P $\beta 6$ and PANC0403 $\alpha v \beta 6$ positive cell lines. This increased uptake of t-L led to an increased therapeutic efficacy of t-L-ALD at sensitising A375P $\beta 6$ to $\gamma \delta$ T cells when compared to L-ALD. The amount of receptor present on the surface of cells is a key consideration when evaluating a targeted drug delivery system. The expression of $\alpha v \beta 6$ receptor on A375P $\beta 6$ cells was confirmed *in vivo* in a flank mouse tumour model in a previous study carried out by co-authors of this paper. SPECT/CT imaging showed that the radiolabelled peptide A20FMDV2 had seven times higher retention in the $\alpha v \beta 6$ positive A375P $\beta 6$ solid tumours than the $\alpha v \beta 6$ negative A375Ppuro tumour implanted in the same mouse (Saha et al., 2010). This demonstrates the expression of the $\alpha v \beta 6$ receptor *in vivo*. In our study, it has been shown that the targeting efficiency of t-L was linked to $\alpha v \beta 6$ integrin receptor expression on the cell surface. As

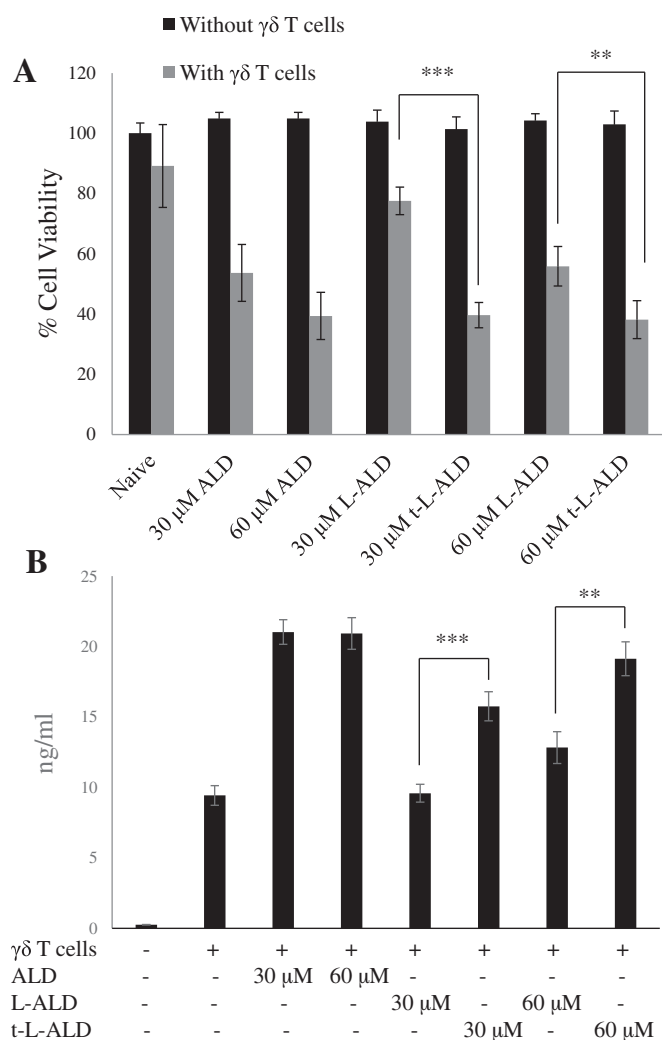


Fig. 3. The ability of L-ALD and t-L-ALD to activate $\gamma\delta$ T cells. (A) Cells were treated with ALD, L-ALD or t-L-ALD for 24 h at 30 or 60 μ M for 24 h. The treatments were then removed and replaced with 2×10^5 $\gamma\delta$ T cells for a further 24 h before a MTT assay was performed. t-L-ALD increased the sensitivity of A375P β 6 cells to $\gamma\delta$ T cells compared to L-ALD (grey bars). ALD, L-ALD or t-L-ALD did not cause cytotoxicity alone at the concentrations used (black bars). (B) IFN- γ ELISA was performed on supernatant removed prior to the MTT assay. t-L-ALD led to higher release of IFN- γ from $\gamma\delta$ T cells than L-ALD. Data was expressed as means \pm SD ($n = 5$). ** $P < 0.01$, *** $P < 0.001$, (Student's t-test L-ALD vs. t-L-ALD).

expected, the targeting efficiency was directly proportional the level of receptor expression, when comparing the three $\alpha\beta$ 6 positive cell lines with A375P β 6 > PANC0403 > 4T1 in terms of both $\alpha\beta$ 6 integrin receptor expression and targeting efficiency. This correlation has been previously reported by Elias et al. [33], with the density of the cell-surface HER2/neu receptor shown to be an important factor in the targeting capability of HER2-targeted nanoparticles.

While the peptide A20FMDV2 has previously been shown to selectively target the integrin receptor $\alpha\beta$ 6 *in vivo* [12,13,34], it has not been conjugated to a nanoparticle before. In this work we provide evidence of successful conjugation of the peptide A20FMDV2 to the surface of liposomes for the first time, and have shown using *in vitro* peptide inhibition studies that the t-L are taken up by cells in a receptor-specific manner. Only one study by Grey et al. has specifically targeted the $\alpha\beta$ 6 integrin receptor using a liposomal formulation [14]. In this study, liposomes were conjugated to the $\alpha\beta$ 6-specific peptide, H2009.1. Interestingly, authors have shown that *in vitro* targeting using the $\alpha\beta$ 6-positive cell line, H2009, could be achieved only when the peptide was incorporated in the tetrameric form and not the monomeric

form. Our results have shown that *in vitro* targeting could be achieved despite using the monomeric form of the peptide. Future work investigating the use of multivalent forms of the peptide A20FMDV2 to further increase targeting efficiency is therefore worth investigating.

In our study, while active targeting could be achieved *in vitro* using t-L, no increase in %ID/g tumour, could be seen in $\alpha\beta$ 6 positive tumours during *in vivo* bio-distribution analysis. There have been previous reports in the literature demonstrating that peptide-targeted liposomes showed no improvement in tumour accumulation compared to untargeted liposomes *in vivo* [35]. It was therefore not surprising to see comparable tumour uptake data *in vivo* for L and t-L in all tumours tested. However, we hypothesised that targeting L-ALD to the $\alpha\beta$ 6 integrin receptor, known to be overexpressed on cancer cells and absent on healthy cells, will result in increased uptake of t-L-ALD due to receptor-mediated endocytosis *in vivo* and hence better therapeutic outcomes, when combined with $\gamma\delta$ T cell-based immunotherapy. Kirpotin et al. demonstrated that despite no increase in tumour uptake of HER2 targeted liposomes in subcutaneous HER-2 positive breast cancer tumours *in vivo*, when excised tumours were studied using flow cytometry and microscopy, a 6-fold increase in cell internalisation of these targeted liposomes was observed [36]. Similarly, in another study, transferrin-targeted siRNA nanoparticles did not show an increase in tumour accumulation but resulted in a ~50% decrease in tumour growth compared to non-targeted nanoparticles due to increased cellular uptake [37]. Our therapy in experimental metastatic melanoma A375P β 6-lung model results showed no added advantage using t-L-ALD over L-ALD when used in combination with $\gamma\delta$ T cells, following our treatment protocols. There could be several explanations to the results obtained; the most obvious one is that L-ALD, in combination with immunotherapy, resulted in efficient tumour growth delay, decreasing the scope for any further improvements, using the targeted delivery approach to be detected. Using lower doses of L-ALD and t-L-ALD may reveal a difference in therapeutic efficacy of the two formulations. Additionally, when L-ALD and t-L-ALD were used as monotherapies, mice treated with t-L-ALD had an average tumour size that was 2.6 times lower than that of mice treated with L-ALD. We hypothesise that this may be as results of higher affinity of t-L-ALD than L-ALD to A375P β 6 cells as demonstrated during *in vitro* studies. Another possibility could be that ALD experiences better endosomal escape from t-L-ALD than L-ALD, facilitated by the receptor-mediated uptake of the former. Unfortunately however, large variations in tumour size meant that this reduction in tumour size was not significant. Using higher doses of L-ALD and t-L-ALD as monotherapies or increasing the number of mice per treatment group may allow the difference in therapeutic efficacy to be observed.

The lack of correlation between the *in vitro* and *in vivo* targeting efficacy that we observed agrees with a previous study by Gray et al. [14]. As discussed above, liposomes targeted using the $\alpha\beta$ 6-specific peptide H2009 in its tetrameric form demonstrated encouraging findings *in vitro*, with a 5–10 fold increase in uptake for targeted liposome. However, targeted liposomes did not lead to an improvement in targeting or efficacy *in vivo* using an $\alpha\beta$ 6 positive H2009 subcutaneous tumour model [35]. Gray and his colleagues, concluded that it is the properties of the liposome (size and PEGylation) and not the targeting peptide that determines *in vivo* bio-distribution. Poor tumour penetration due to the dense extracellular matrix and high interstitial pressure in solid tumours may have prevented liposomes from exerting a targeting effect within the tumour itself [38,39]. Likewise, a folate-targeted formulation of L-ALD demonstrated *in vitro* targeting but no therapeutic advantage was observed during *in vivo* studies with a folate receptor- α positive ovarian tumour model [24]. The presence of folate receptors on endogenous non-tumour cells leading to accelerated systemic clearance was hypothesised to be responsible for the lower therapeutic efficacy of the targeted formulation.

Recent studies have revealed that the formation of a protein corona on the surface of liposomes can lead to an inhibition of targeting

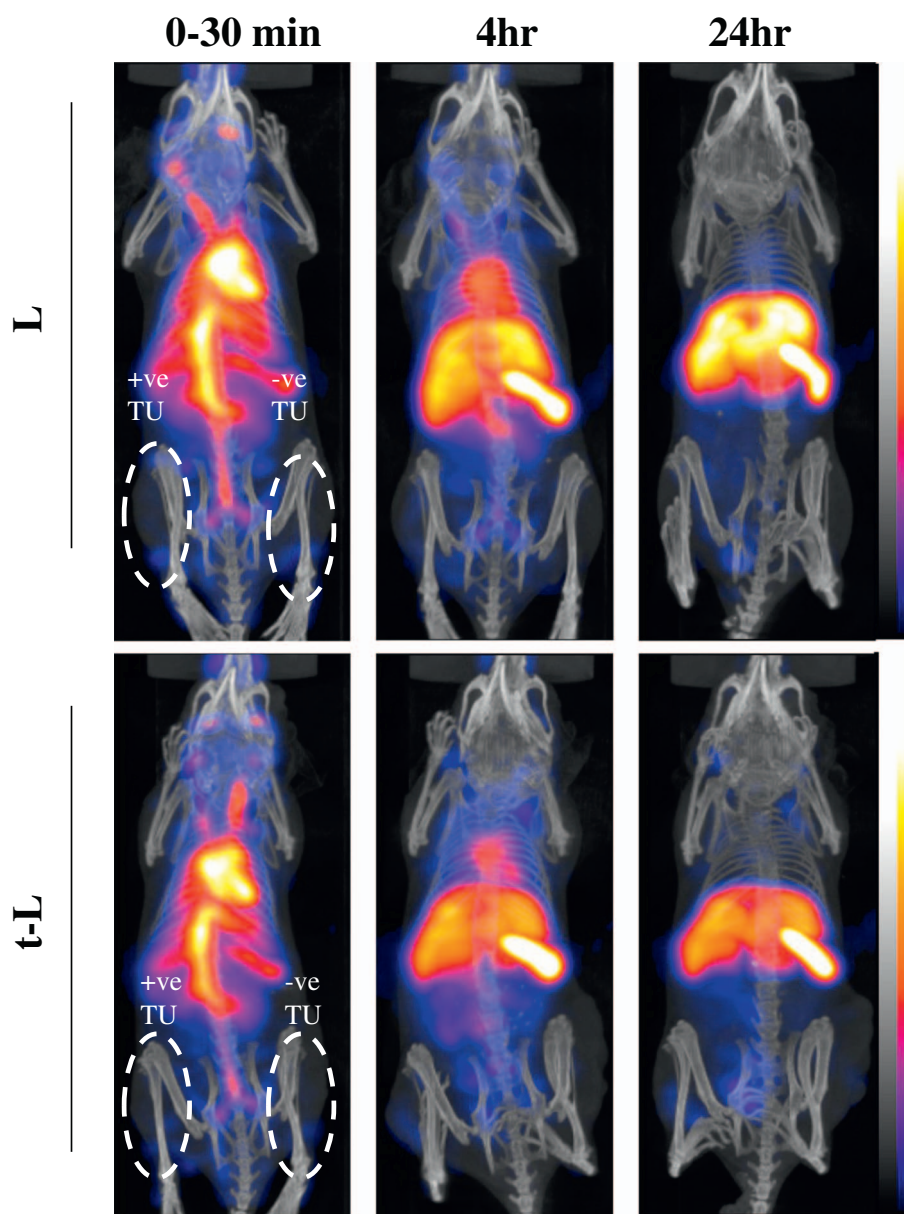


Fig. 4. *In vivo* whole body 3D SPECT/CT imaging of ^{111}In labelled liposomes in tumour-bearing immunocompromised mice. Mice were i.v. injected with ^{111}In labelled liposomes at a dose of $2\ \mu\text{mol}$ lipid/mouse. Mice were inoculated bi-focally with the $\alpha\text{v}\beta 6$ positive tumour on the left of the image (A375P $\beta 6$) (right flank) and the negative tumour (A375Ppuro) on the right of the image (left flank). Whole body 3D SPECT/CT imaging were performed at 0–30 min, 4 and 24 h post-injection with scanning time of 40–60 min each. SPECT data is displayed in colour scale and CT data is in grey scale, respectively (high to low signals: top to bottom).

efficacy, as the targeting-peptides can be hidden from their receptors [40–43]. We have therefore conducted a study to see if incubation of t-L-ALD with mouse serum will compromise the targeting efficiency, in an attempt to correlate the *in vitro* targeting efficiency with *in vivo* active targeting in a living mouse. Our results indeed showed that incubation with mouse serum reduced the targeting efficiency of t-L, in a time-dependent manner. This suggests that the direct interaction of mouse serum and t-L adversely affects active targeting of t-L-ALD. Further studies to explore types of protein corona involved are warranted and as it has been reported that protein corona may differ based on what species the serum is from, extrapolation of data in mice to humans is not possible [40]. Another explanation of the mouse serum data could be the enzymatic degradation of A20FMDV2. A study performed by Saha et al. has shown that only 50% of the peptide A20FMDV2 [13] remained intact after 4 h incubation with mouse serum. Amino acid modifications may help improve resistance to enzymatic degradation [44–46]. To understand the exact effect of

serum on active targeting in our study needs further investigation.

5. Conclusion

In this work, A20FMDV2 peptide was successfully conjugated to PEGylated liposomes and active targeting was confirmed *in vitro* in melanoma and pancreatic cell lines. *In vitro* targeting efficiency was directly linked to levels of $\alpha\text{v}\beta 6$ receptor expressions and was blocked by addition of excess peptide, suggesting receptor-mediated endocytosis as a mechanism of internalisation. $\alpha\text{v}\beta 6$ -targeted liposomal alendronate led to significant improvement in sensitisation of $\alpha\text{v}\beta 6$ positive cancer cell line to $\gamma\delta$ T cells, and improved cell kill *in vitro*. Despite the slight promise in using t-L-ALD as a monotherapy, no added advantage was observed when combined with $\gamma\delta$ T cells immunotherapy, in an experimental metastatic lung mice model. Future therapy studies with modified treatment protocols need to be performed to determine if a significant improvement in therapeutic efficacy using t-L-ALD can be

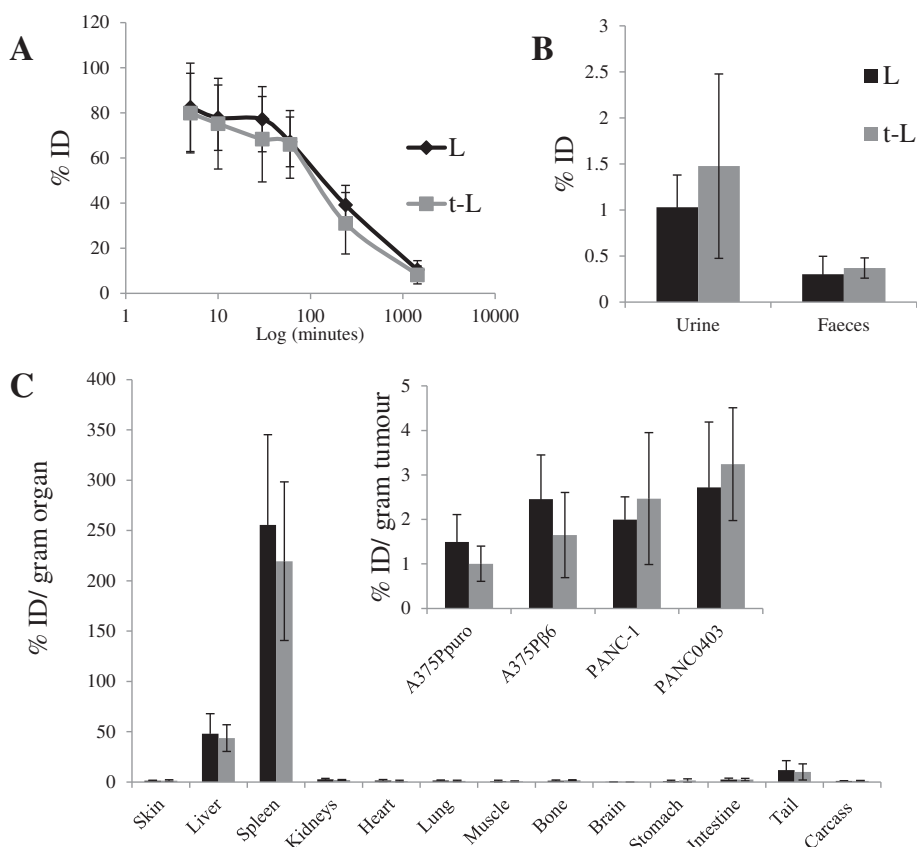


Fig. 5. *In vivo* bio-distribution of radiolabelled L and t-L in tumour bearing SCID/Beige mice after single dose administration via tail vein injection. (A) Blood clearance profile of liposomes expressed as %ID. (B) Excretion profile of liposomes after 24 h expressed as %ID. (C) Results were expressed as percentage injected dose per gram of organ (%ID/g organ) at 24 h after injection of 2 μmol liposome/mouse. Organ biodistribution data were taken from mice bearing A375Ppuro and A375Pβ6 tumours. No significant difference between the bio-distribution of the untargeted and targeted liposomes was seen. Data was expressed as means ± SD (n = 3).

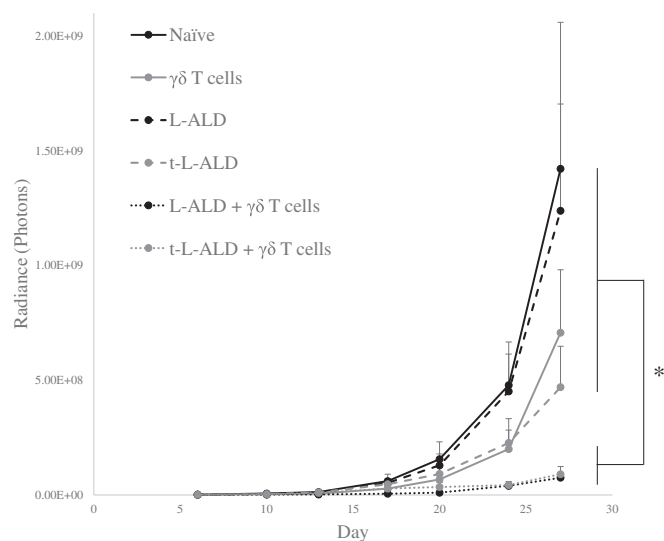


Fig. 6. *In vivo* tumour therapy study. Experimental metastatic lung A375Pβ6 tumour bearing mice were treated intravenously on day 6 with L-ALD, t-L-ALD (0.5 μmol ALD/mouse), 1 × 10⁷ γδ T cells/mouse or were pre-treated with L-ALD or t-L-ALD 24 h prior to injection of γδ T cells. Three similar treatments were given intravenously at one week intervals, commencing on day 6 post-tumour inoculation. Tumour progression was monitored by bioluminescence imaging. A significant reduction in tumour growth was observed for the L-ALD/γδ and t-L-ALD/γδ combinatory immunotherapy groups compared to control mice or those treated with monotherapy of γδ T cells, L-ALD or t-L-ALD. t-L-ALD monotherapy resulted in an inhibition of tumour growth but this was not significant (p = 0.15). Data was expressed as mean ± SEM (n = 7). *p < 0.05, (ANOVA).

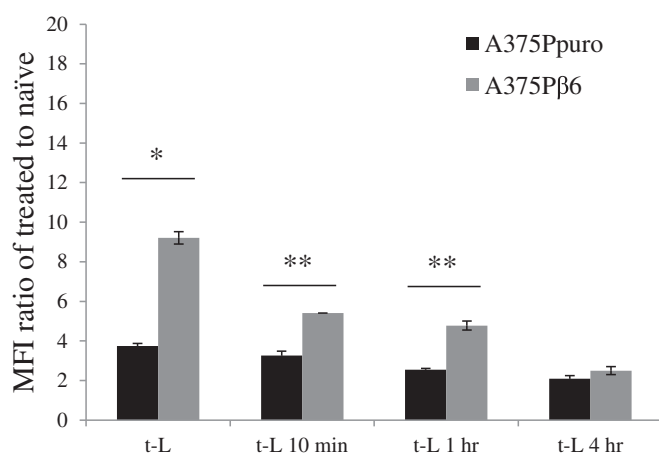


Fig. 7. Effect of incubation of t-L with mouse serum on targeting efficacy. t-L were exposed to mouse serum for various lengths of times (10 min, 1 h, 4 h). The melanoma cell lines, A375Ppuro and A375Pβ6 were incubated with these liposomes for 1 h. Results are displayed as the MFI fold increase of naive cells. Incubation of t-L with mouse serum leads to a reduction in receptor-mediated uptake cell uptake in the αvβ6 positive A375Pβ6 cell line. Cellular uptake was assessed by measuring the MFI using flow cytometry and FL-1 detector. Values are expressed as mean ± SD (n = 3). *p < 0.05, **p < 0.01, (Student's t-test A375Ppuro vs. A375Pβ6).

achieved. *In vivo* peptide stability and the protein corona effect may be responsible for the decrease in *in vivo* targeting efficacy compared to the *in vitro* results obtained, which also needs to be investigated further.

Acknowledgements

K. Al-Jamal acknowledges funding from BBSRC (BB/J008656/1) and Worldwide Cancer Research (12 – 1054). N. Hodgins is a recipient of Graduate School King's Health Partner's scholarship. W. Al-Jamal acknowledges funding from Prostate Cancer UK (Grant CDF-12-002) and (EPSRC) (EP/M008657/1). J. Maher acknowledges support from the Experimental Cancer Medicine Centre at King's College London and the National Institute for Health Research (NIHR) Biomedical Research Centre based at Guy's and St Thomas' NHS Foundation Trust and King's College London. The views expressed are those of the authors and not necessarily those of the NHS, the NIHR or the Department of Health. Pedro M. Costa is a Sir Henry Wellcome Post-doctoral fellow [WT103913].

Appendix A. Supplementary data

Supplementary data to this article can be found online at <http://dx.doi.org/10.1016/j.jconrel.2017.04.025>.

References

- M. Agrez, A. Chen, R.I. Cone, R. Pytela, D. Sheppard, The alpha v beta 6 integrin promotes proliferation of colon carcinoma cells through a unique region of the beta 6 cytoplasmic domain, *J. Cell Biol.* 127 (1994) 547–556.
- Z. Zhao-Yang, X. Ke-Sen, H. Qing-Si, N. Wei-Bo, W. Jia-Yong, M. Yue-Tang, W. Jin-Shen, W. Guo-Qiang, Y. Guang-Yun, N. Jun, Signaling and regulatory mechanisms of integrin alphavbeta6 on the apoptosis of colon cancer cells, *Cancer Lett.* 266 (2008) 209–215.
- Q. Sun, F. Sun, B. Wang, S. Liu, W. Niu, E. Liu, C. Peng, J. Wang, H. Gao, B. Liang, Z. Niu, X. Zou, J. Niu, Interleukin-8 promotes cell migration through integrin alphavbeta6 upregulation in colorectal cancer, *Cancer Lett.* 354 (2014) 245–253.
- G.Y. Yang, S. Guo, C.Y. Dong, X.Q. Wang, B.Y. Hu, Y.F. Liu, Y.W. Chen, J. Niu, J.H. Dong, Integrin alphavbeta6 sustains and promotes tumor invasive growth in colon cancer progression, *World J. Gastroenterol.* 21 (2015) 7457–7467.
- J.M. Breuss, J. Gallo, H.M. DeLisser, I.V. Klimanskaya, H.G. Folkesson, J.F. Pittet, S.L. Nishimura, K. Aldape, D.V. Landers, W. Carpenter, et al., Expression of the beta 6 integrin subunit in development, neoplasia and tissue repair suggests a role in epithelial remodeling, *J. Cell Sci.* 108 (Pt 6) (1995) 2241–2251.
- K. Haapasalmi, K. Zhang, M. Tonnesen, J. Olerud, D. Sheppard, T. Salo, R. Kramer, R.A. Clark, V.J. Uitto, H. Larjava, Keratinocytes in human wounds express alpha v beta 6 integrin, *J. Invest. Dermatol.* 106 (1996) 42–48.
- R.C. Bates, D.I. Bellovin, C. Brown, E. Maynard, B. Wu, H. Kawakatsu, D. Sheppard, P. Oettgen, A.M. Mercurio, Transcriptional activation of integrin beta6 during the epithelial-mesenchymal transition defines a novel prognostic indicator of aggressive colon carcinoma, *J. Clin. Invest.* 115 (2005) 339–347.
- A. Kawashima, S. Tsugawa, A. Boku, M. Kobayashi, T. Minamoto, I. Nakanishi, Y. Oda, Expression of alphav integrin family in gastric carcinomas: increased alphavbeta6 is associated with lymph node metastasis, *Pathol. Res. Pract.* 199 (2003) 57–64.
- J. Jones, F.M. Watt, P.M. Speight, Changes in the expression of alpha v integrins in oral squamous cell carcinomas, *J. Oral Pathol. Med.* 26 (1997) 63–68.
- G.J. Thomas, M.P. Lewis, I.R. Hart, J.F. Marshall, P.M. Speight, AlphaVbeta6 integrin promotes invasion of squamous carcinoma cells through up-regulation of matrix metalloproteinase-9, *Int. J. Cancer* 92 (2001) 641–650.
- G.J. Thomas, M.P. Lewis, S.A. Whawell, A. Russell, D. Sheppard, I.R. Hart, P.M. Speight, J.F. Marshall, Expression of the alphavbeta6 integrin promotes migration and invasion in squamous carcinoma cells, *J. Invest. Dermatol.* 117 (2001) 67–73.
- D. DiCara, C. Rapisarda, J.L. Sutcliffe, S.M. Violette, P.H. Weinreb, I.R. Hart, M.J. Howard, J.F. Marshall, Structure-function analysis of Arg-Gly-Asp helix motifs in alpha v beta 6 integrin ligands, *J. Biol. Chem.* 282 (2007) 9657–9665.
- A. Saha, D. Ellison, G.J. Thomas, S. Vallath, S.J. Mather, I.R. Hart, J.F. Marshall, High-resolution in vivo imaging of breast cancer by targeting the pro-invasive integrin alphavbeta6, *J. Pathol.* 222 (2010) 52–63.
- B.P. Gray, S. Li, K.C. Brown, From phage display to nanoparticle delivery: functionalizing liposomes with multivalent peptides improves targeting to a cancer biomarker, *Bioconjug. Chem.* 24 (2013) 85–96.
- S.R. Mattarollo, T. Kenna, M. Nieda, A.J. Nicol, Chemotherapy and zoledronate sensitize solid tumour cells to Vgamma9Vdelta2 T cell cytotoxicity, *Cancer Immunol. Immunother.* 56 (2007) 1285–1297.
- E. Cimini, P. Piacentini, A. Sacchi, C. Gioia, S. Leone, G.M. Lauro, F. Martini, C. Agrati, Zoledronic acid enhances Vdelta2 T-lymphocyte antitumor response to human glioma cell lines, *Int. J. Immunopathol. Pharmacol.* 24 (2011) 139–148.
- A. Hoh, A. Dewerth, F. Vogt, J. Wenz, P.A. Baeuerle, S.W. Warmann, J. Fuchs, S. Armeanu-Ebinger, The activity of gammadelta T cells against paediatric liver tumour cells and spheroids in cell culture, *Liver Int.* 33 (2013) 127–136.
- Z. Li, H. Peng, Q. Xu, Z. Ye, Sensitization of human osteosarcoma cells to Vgamma9Vdelta2 T-cell-mediated cytotoxicity by zoledronate, *J. Orthop. Res.* 30 (2012) 824–830.
- N. Nishio, M. Fujita, Y. Tanaka, H. Maki, R. Zhang, T. Hirosawa, A. Demachi-Okamura, Y. Uemura, O. Taguchi, Y. Takahashi, S. Kojima, K. Kuzushima, Zoledronate sensitizes neuroblastoma-derived tumor-initiating cells to cytotoxicity mediated by human gammadelta T cells, *J. Immunother.* 35 (2012) 598–606.
- I. Benzaid, H. Monkkonen, E. Bonnelye, J. Monkkonen, P. Clezardin, In vivo phosphoantigen levels in bisphosphonate-treated human breast tumors trigger Vgamma9Vdelta2 T-cell antitumor cytotoxicity through ICAM-1 engagement, *Clin. Cancer Res.* 18 (2012) 6249–6259.
- I. Benzaid, H. Monkkonen, V. Stresing, E. Bonnelye, J. Green, J. Monkkonen, J.L. Touraine, P. Clezardin, High phosphoantigen levels in bisphosphonate-treated human breast tumors promote Vgamma9Vdelta2 T-cell chemotaxis and cytotoxicity in vivo, *Cancer Res.* 71 (2011) 4562–4572.
- E. Di Carlo, P. Bocca, L. Emionite, M. Cilli, G. Cipollone, F. Morandi, L. Raffaghello, V. Pistoia, I. Prigione, Mechanisms of the antitumor activity of human Vgamma9Vdelta2 T cells in combination with zoledronic acid in a preclinical model of neuroblastoma, *Mol. Ther.* 21 (2013) 1034–1043.
- D. Kabelitz, D. Wesch, E. Pitters, M. Zoller, Characterization of tumor reactivity of human V gamma 9V delta 2 gamma delta T cells in vitro and in SCID mice in vivo, *J. Immunol.* 173 (2004) 6767–6776.
- A.C. Parente-Pereira, H. Shmeeda, L.M. Whilding, C.P. Zambirinis, J. Foster, S.J. van der Stegen, R. Beatson, T. Zabinski, N. Brewig, J.K. Sosabowski, S. Mather, S. Ghaem-Maghani, A. Gabizon, J. Maher, Adoptive immunotherapy of epithelial ovarian cancer with Vgamma9Vdelta2 T cells, potentiated by liposomal alendronic acid, *J. Immunol.* 193 (2014) 5557–5566.
- T. Santolaria, M. Robard, A. Leger, V. Catros, M. Bonneville, E. Scotet, Repeated systemic administrations of both aminobisphosphonates and human Vgamma9Vdelta2 T cells efficiently control tumor development in vivo, *J. Immunol.* 191 (2013) 1993–2000.
- K. Sato, S. Kimura, H. Segawa, A. Yokota, S. Matsumoto, J. Kuroda, M. Nogawa, T. Yuasa, Y. Kiyono, H. Wada, T. Maekawa, Cytotoxic effects of gammadelta T cells expanded ex vivo by a third generation bisphosphonate for cancer immunotherapy, *Int. J. Cancer* 116 (2005) 94–99.
- T. Yuasa, K. Sato, E. Ashihara, M. Takeuchi, S. Maita, N. Tsuchiya, T. Habuchi, T. Maekawa, S. Kimura, Intravesical administration of gammadelta T cells successfully prevents the growth of bladder cancer in the murine model, *Cancer Immunol. Immunother.* 58 (2009) 493–502.
- H. Maeda, The enhanced permeability and retention (EPR) effect in tumor vasculature: the key role of tumor-selective macromolecular drug targeting, *Adv. Enzym. Regul.* 41 (2001) 189–207.
- R. New, *Liposomes: A Practical Approach*, (1990).
- K.T. Al-Jamal, A. Nunes, L. Methven, H. Ali-Boucetta, S. Li, F.M. Toma, M.A. Herrero, W.T. Al-Jamal, H.M. ten Eikelder, J. Foster, S. Mather, M. Prato, A. Bianco, K. Kostarelos, Degree of chemical functionalization of carbon nanotubes determines tissue distribution and excretion profile, *Angew. Chem. Int. Ed.* 51 (2012) 6389–6393.
- I. Millet, E. Bouic-Pages, D. Hoa, D. Azria, P. Taourel, Growth of breast cancer recurrences assessed by consecutive MRI, *BMC Cancer* 11 (2011) 155.
- K. Maruyama, Intracellular targeting delivery of liposomal drugs to solid tumors based on EPR effects, *Adv. Drug Deliv. Rev.* 63 (2011) 161–169.
- D.R. Elias, A. Poloukhine, V. Popik, A. Tsourkas, Effect of ligand density, receptor density, and nanoparticle size on cell targeting, *Nanomedicine* 9 (2013) 194–201.
- H. Kogelberg, B. Tolner, G.J. Thomas, D. Di Cara, S. Minogue, B. Ramesh, S. Sodha, D. Marsh, M.W. Lowdell, T. Meyer, R.H. Begent, I. Hart, J.F. Marshall, K. Chester, Engineering a single-chain Fv antibody to alpha v beta 6 integrin using the specificity-determining loop of a foot-and-mouth disease virus, *J. Mol. Biol.* 382 (2008) 385–401.
- B.P. Gray, M.J. McGuire, K.C. Brown, A liposomal drug platform overrides peptide ligand targeting to a cancer biomarker, irrespective of ligand affinity or density, *PLoS One* 8 (2013) e72938.
- D.B. Kirpotin, D.C. Drummond, Y. Shao, M.R. Shalaby, K. Hong, U.B. Nielsen, J.D. Marks, C.C. Benz, J.W. Park, Antibody targeting of long-circulating lipidic nanoparticles does not increase tumor localization but does increase internalization in animal models, *Cancer Res.* 66 (2006) 6732–6740.
- D.W. Bartlett, H. Su, I.J. Hildebrandt, W.A. Weber, M.E. Davis, Impact of tumor-specific targeting on the biodistribution and efficacy of siRNA nanoparticles measured by multimodality in vivo imaging, *Proc. Natl. Acad. Sci. U. S. A.* 104 (2007) 15549–15554.
- R.K. Jain, Transport of molecules in the tumor interstitium: a review, *Cancer Res.* 47 (1987) 3039–3051.
- P.A. Netti, D.A. Berk, M.A. Swartz, A.J. Grodzinsky, R.K. Jain, Role of extracellular matrix assembly in interstitial transport in solid tumors, *Cancer Res.* 60 (2000) 2497–2503.
- G. Caracciolo, Liposome-protein corona in a physiological environment: challenges and opportunities for targeted delivery of nanomedicines, *Nanomedicine* 11 (2015) 543–557.
- R. Safavi-Sohi, S. Maghari, M. Raoufi, S.A. Jalali, M.J. Hajipour, A. Ghassempour, M. Mahmoudi, Bypassing protein corona issue on active targeting: zwitterionic coatings dictate specific interactions of targeting moieties and cell receptors, *ACS Appl. Mater. Interfaces* 8 (35) (2016) 22808–22818.
- A. Salvati, A.S. Pitek, M.P. Monopoli, K. Prapainop, F.B. Bombelli, D.R. Hristov, P.M. Kelly, C. Aberg, E. Mahon, K.A. Dawson, Transferrin-functionalized nanoparticles lose their targeting capabilities when a biomolecule corona adsorbs on the surface, *Nat. Nanotechnol.* 8 (2013) 137–143.
- V. Mirshafiee, M. Mahmoudi, K.Y. Lou, J.J. Cheng, M.L. Kraft, Protein corona significantly reduces active targeting yield, *Chem. Commun.* 49 (2013) 2557–2559.

- [44] A.A. Stromstedt, M. Pasupuleti, A. Schmidtchen, M. Malmsten, Evaluation of strategies for improving proteolytic resistance of antimicrobial peptides by using variants of EFK17, an internal segment of LL-37, *Antimicrob. Agents Chemother.* 53 (2009) 593–602.
- [45] R. Galati, A. Verdina, G. Falasca, A. Chersi, Increased resistance of peptides to serum proteases by modification of their amino groups, *Z. Naturforsch.* 58 (2003) 558–561.
- [46] M.T. Weinstock, J.N. Francis, J.S. Redman, M.S. Kay, Protease-resistant peptide design-empowering nature's fragile warriors against HIV, *Biopolymers* 98 (2012) 431–442.